X-621-67-422

NASA TM X-55903

THE STATISTICAL MEASUREMENT OF SPECTRAL AMPLITUDES AND PHASES OF ATMOSPHERICS IN THE VLF RANGE

H. VOLLAND
G. HEYDT
W. HARTH

AUGUST 1967

GODDARD SPACE FLIGHT CENTER
GREENBELT, MARYLAND

THE STATISTICAL MEASUREMENT OF SPECTRAL AMPLITUDES AND PHASES OF ATMOSPHERICS IN THE VLF RANGE*

H. Volland**
Goddard Space Flight Center

G. Heydt
Heinrich-Hertz Institut
Berlin-Charlottenburg
Germany

and

W. Harth
Astronomical Institutes
Bonn University, Germany

* Prepared for the 13th Symposium of the AGARD ELECTROMAGNETIC WAVE PROPAGATION COMMITTEE on "Phase and Frequency Instability in Electromagnetic Wave Propagation" in Ankara, Turkey, 9th - 12th October, 1967

** On leave from the Astronomical Institutes of the University of Bonn, Germany, as a National Academy of Sciences-National Research Council Associate with the National Aeronautics and Space Administration.

August 1967

GODDARD SPACE FLIGHT CENTER
Greenbelt, Maryland

Abstract

An equipment has been developed at the Heinrich-Hertz-Institut in Berlin which within the VLF range allows the measurement of the statistical spectral amplitude distribution, the ratio of the spectral amplitude at two different frequencies and the statistical group time delay of the phase of the spectral amplitude, of atmospherics coming from discrete thunderstorms. The group time delay is directly related to the phase of the propagation function within the atmospheric waveguide and depends on distance, azimuth, frequency, and effective height of the waveguide. Its variations with frequency and time have been measured for different thunderstorms. They give evidence of the time change of the ionospheric reflection characteristics within the VLF range. Since the registrations depend on the azimuth of the incoming atmospherics, thunderstorms can be located from the group time-delay measurements. Moreover, the statistical treatment of the atmospherics allows a quantitative determination of the number of lightning flashes within the thunderstorm.

CONTENTS

1. Introduction

Atmospherics are electromagnetic impulses generated by lightning discharges and propagating within the waveguide formed by the earth's surface and the lower ionosphere. The spectrum of an atmospheric is rather broad with a maximum in the VLF range. The impulse becomes dispersed during its propagation in the waveguide, Observation of atmospherics provides the following information:

1. The impulse form of the lightning discharges at the origin.

2. The number of impulses and impulse series of the lightning discharges as dependent on geographical location and time.

3. The time-, space-, and frequency-dependent transmission function of the aforesaid waveguide formed by earth and ionosphere.

Lightning discharges originate according to meteorological conditions. About 100 discharges per second are generated on the earth's surface. There are some preferred centers of atmospherics (e.g. , South America and Africa) and preferred times of day of occurrence (e.g. , late afternoon in middle Europe) (Reference 1). The impulse series is almost arbitrary but shows some repetition frequency (Reference 2). The amplitudes of the discharges are statistically distributed.

This nature of atmospherics suggests a statistical spectral method for their measurement. Fortunately, the sources of atmospherics usually are thunderstorms of limited area. Therefore, a method combining direction finding with statistics gives the maximum information when applied to the three points mentioned above.

The Heinrich-Hertz-Institut in Berlin-Charlottenburg contains an equipment that measures the spectral amplitude, the ratio of the spectral amplitudes, and the group time delay of atmospherics at different azimuths. This equipment is described in section 2. Section 3 gives a brief survey of the measurement of: the impulse form at the origin, the location and number of lightning discharges, and the amplitude of the transmission function of the waveguide. Section 4 interprets the group-time-delay measurements. The group time delay is closely related to the phase of the transmission function and therefore complements the information available from atmospherics.

For information about other methods of atmospheric measurement and their results see References 3 and 4.

2. Description of the equipment

The equipment performs the following functions: direction finding, measurement of spectral amplitudes and their ratio, and group time delay, as described below in sections 2.1 through 2.5 and illustrated by Figures 1 through 5. These equipments are contained in a compact unit and can be operated manually or automatically. In manual operation, a polaroid camera is used. Automatic operation is briefly described in section 2.5.

2.1 Direction finder

The direction-finder aerial system consists of a rod antenna and two fixed crossed-loop antennas (Figure 1). An atmospheric arriving at the loop antennas stimulates the two resonance amplifiers K_X and K_Y tuned at 11 kHz. These amplifiers phase-shift the voltage by ± 45 degrees; the difference of the resulting voltages is obtained by the following stage. The difference-voltage amplitude U_φ does not depend on the azimuth. The phase, however,

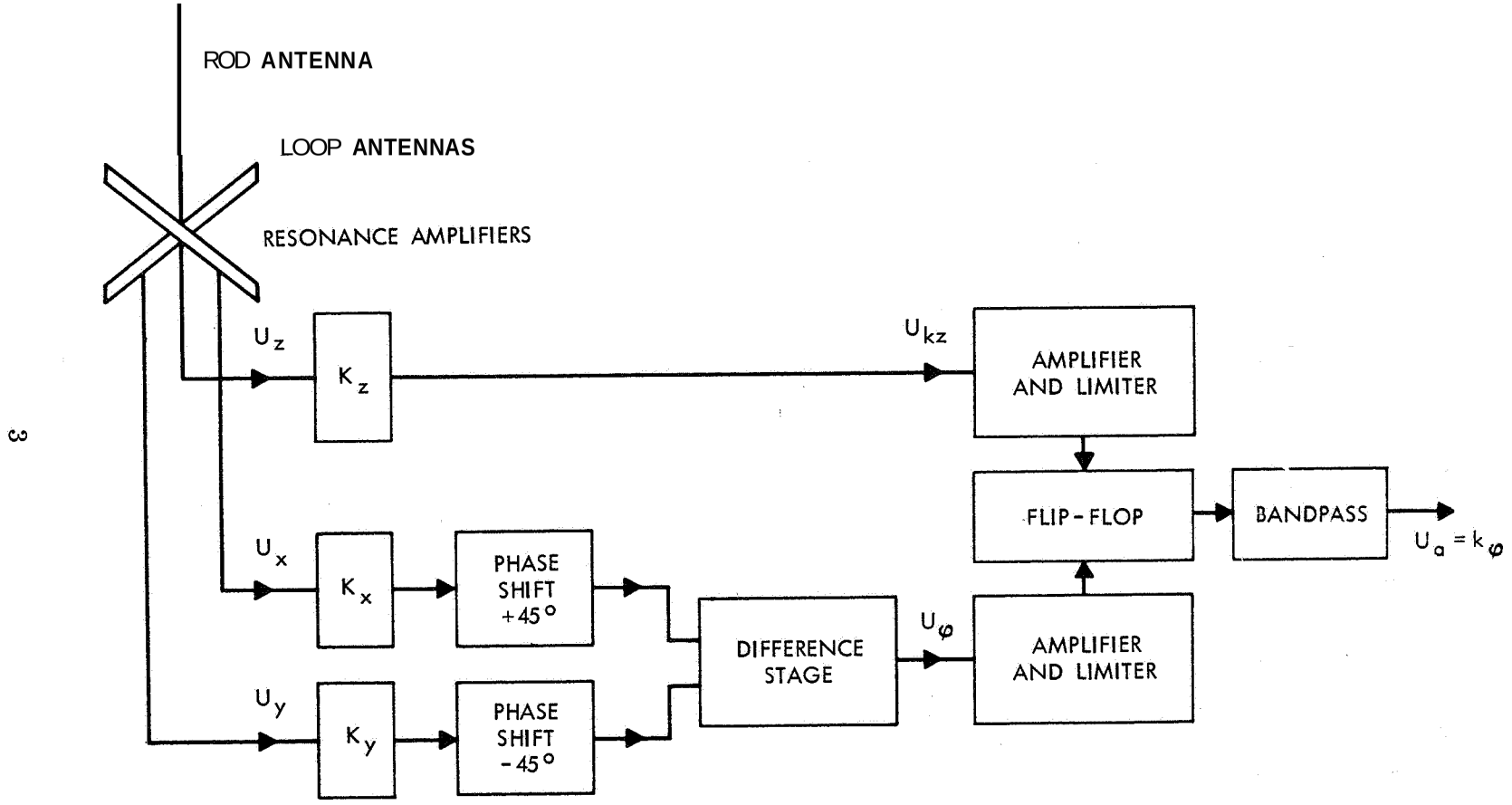

Figure 1 - Direction finder, block diagram.

is proportional to the azimuth φ of the incoming atmospheric, when compared with the output voltage U_{kz} of the third amplifier K_z which is connected with the rod antenna. A phase comparison, therefore, yields a voltage U_a that is proportional to the azimuth of the atmospheric.

2.2 Measurement of spectral amplitudes

A resonance amplifier tunable between 5 and 50 kHz, connected with a rod antenna, measures the vertical component of the spectral electric field strength of an atmospheric. The rectified output voltage U is fed to the X-plates of an oscillograph while the Y-plates are fed by the voltage U_a of the direction finder described in section 2.1. The second differentiation of the output voltage U gives a voltage U_C that so controls the brightness of the X-channel that the U-maximum appears on the oscilloscope screen as a bright spot. Maximum U is proportional to the spectral amplitude of the field strength, and is thus "plotted" against azimuth on the oscilloscope.

Figure 2 shows a photograph of the oscillograph screen exposed for five minutes. Three thunderstorms of different sizes and directions can be separated from the underground noise (which consists of atmospherics from distant thunderstorms).

2.3 Ratio of the spectral amplitudes

For spectral-amplitude ratio measurements, the narrow-band amplifier described in section 2.2 is replaced by two equal amplifiers tuned at different frequencies and combined with a voltage-ratio-measuring unit. The output voltage is a dc pulse, whose height is a unique function of the ratio of the spectral amplitudes at the two frequencies. This unit is again combined with the direction-finder unit and a brightness-control unit. (see Figure 3). Each thunderstorm produces an accumulation of spots; each spot is due to a single lightning discharge.

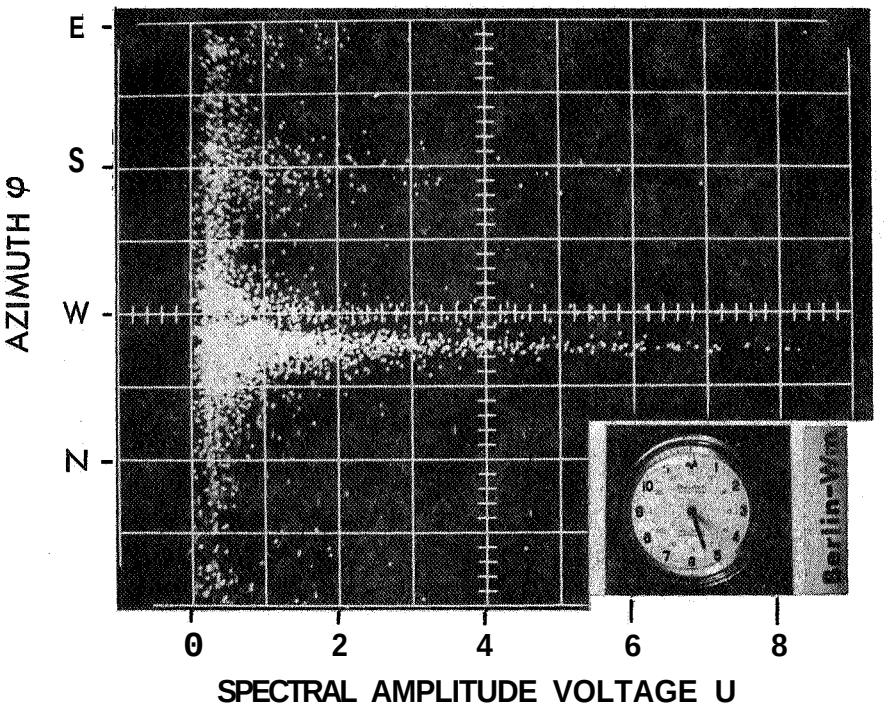

Figure 2 - Oscillograph of spectral amplitude voltage U versus azimuth at 9 kHz (5-minute picture).

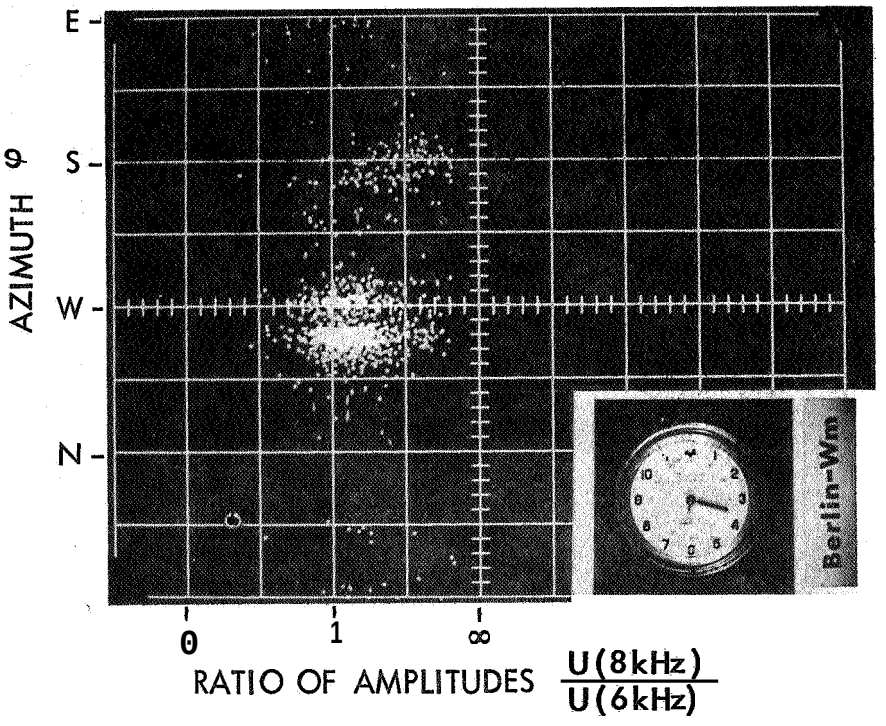

Figure 3 - Oscillograph of spectral amplitude ratio between 6 and 8 kHz versus azimuth (5-minute picture).

2.4 Spectral group time dela

Figure 4 is a block diagram of the equipment for the measurement of group time delay. Three resonance amplifiers are tuned at the frequencies f_m, f_1, and f_2; f_m is an arbitrarily chosen frequency; Δf is an arbitrarily chosen deviation such that

$$f_1 = f_m - \Delta f \qquad (1)$$

$$f_2 = f_m + \Delta f$$

These amplifiers measure field strengths whose phases are Φ_m, Φ_1, and Φ_2. They are stimulated by an atmospheric. The output voltages of the two first stages are mixed. The resulting mixing frequency has the phase $\Phi_1 + \Phi_2$.

In the third stage, the frequency f_m is multiplied, which gives a phase $2\Phi_m$. Both resulting phases are compared in a phase-measuring unit. The output voltage U_g is proportional to the phase difference

$$\Phi_1 + \Phi_2 - 2\Phi_m = -\Delta t_{gr} \Delta\omega \sim \frac{\partial^2 \Phi}{\partial \omega^2} \Delta\omega^2. \qquad (2)$$

That is, it is proportional to the group time delay ($-\Delta t_{gr}$) and to the second derivative of the spectral phase of the atmospheric with respect to the angular frequency $\omega = 2\pi f$.

The voltage U_g is again combined with the voltage U_C of the brightness-control unit and with the voltage U_a of the azimuth of the individual atmospheric. This leads to a measurement as in Figure 5, where thunderstorms of different azimuths and different group time delays can be clearly separated.

2.5 Automatic operation

In automatic operation, the equipment uses an automatic camera recorder. A programmable switching unit manages a regular program of any six kinds

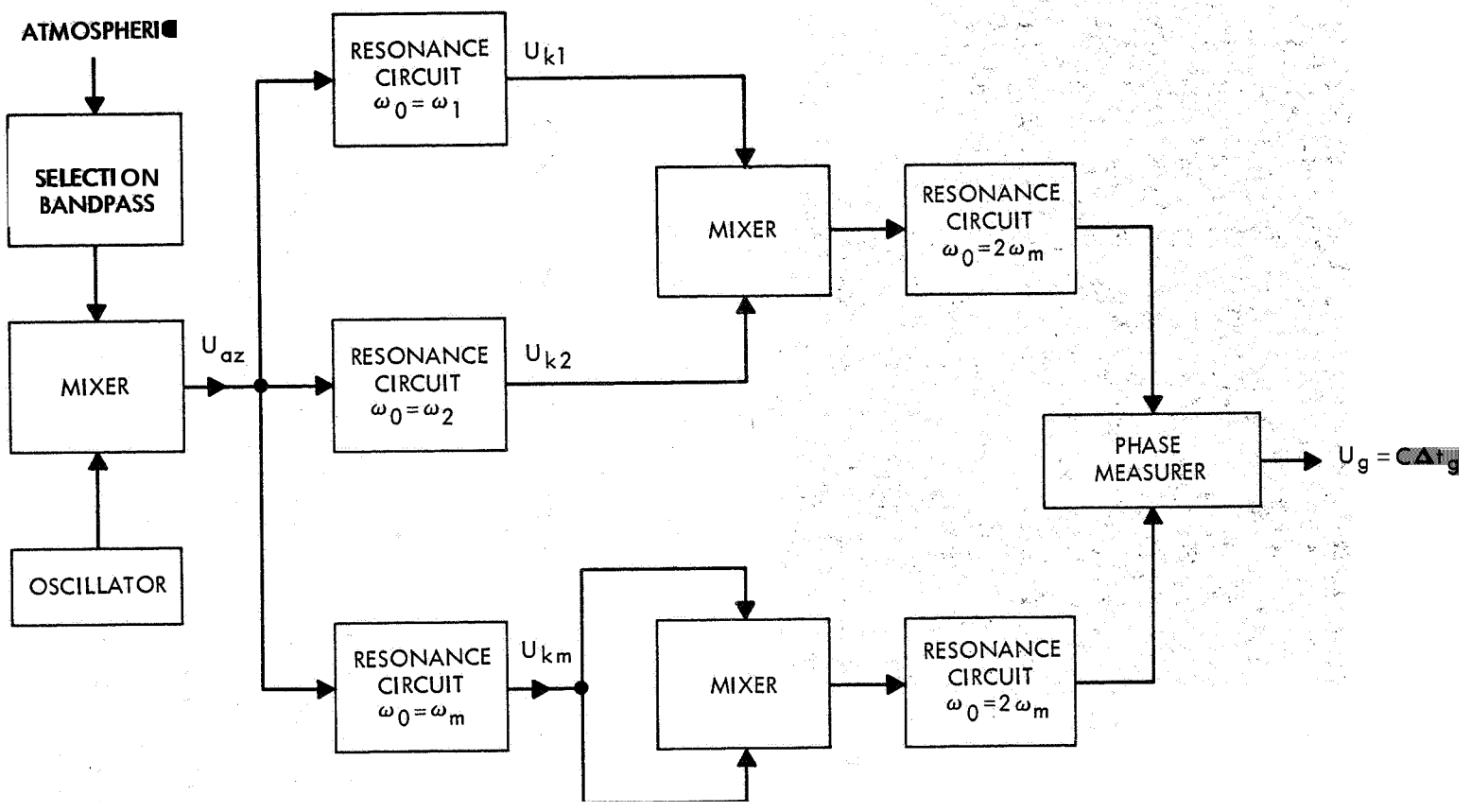

Figure 4 - Group time delay measurement, block diagram.

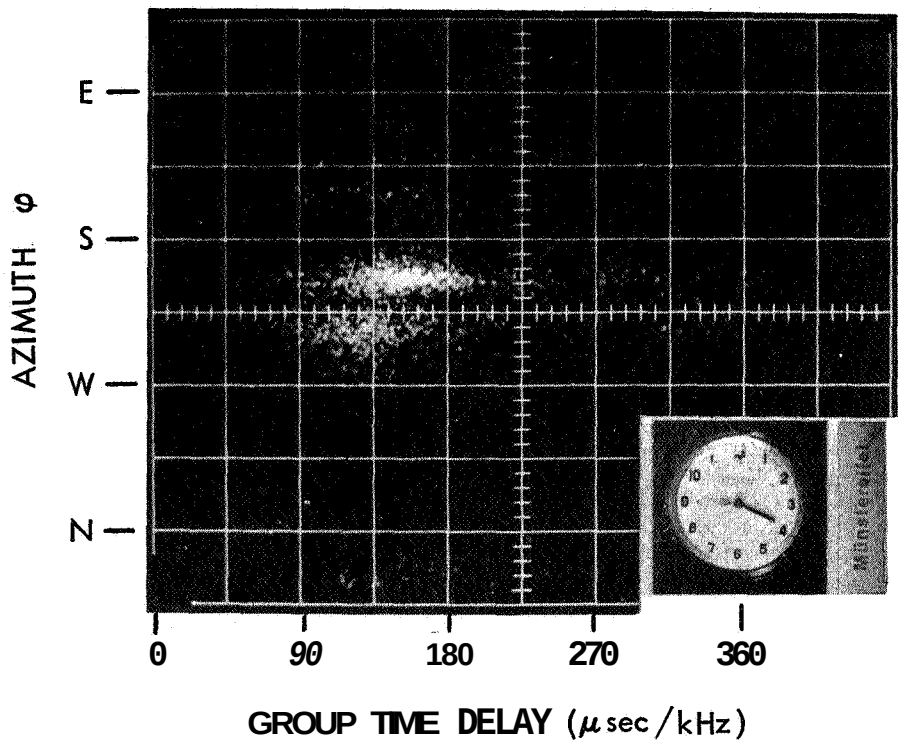

Figure 5 - Oscillograph of group time delay versus azimuth at 6 kHz; bandwidth Δf = 1.4 kHz (5-minute picture).

of measurements which is repeated every hour. For the past year, regular measurements of spectral amplitudes, of the ratio of the spectral amplitudes, and of the group time delay have been performed at three widely spaced places in Germany.

A detailed technical description of this equipment has been given by Heydt (Reference *5)*.

3. Measurement of the spectral electric field strength of the atmospherics

The vertical component of the electric field of a single atmospheric at a distance ρ from its origin can be expressed by the Fourier integral (Reference 6)

$$E(\rho, t) = \int_{-\infty}^{\infty} b(\rho, \omega)\ g(\omega)\ e^{j\{\omega t + \Psi(\rho, \omega) + \psi(\omega)\}}\ d\omega \qquad (3)$$

where ρ = distance, t = time, ω = angular frequency, $B(\rho, \omega) = b\, e^{j\Psi}$ = the transmission function of the waveguide between earth and ionosphere, $G(\omega) = g\, e^{j\psi}$ = the radiative component of the spectral function of the atmospheric at its origin evaluated at distance $\rho = 1$ km.

The equipment described in section 2.2 measures a value proportional to the amplitude of the Fourier component in Equation 3:

$$Ab(\rho, \omega)\ g(\omega).$$

The number of atmospherics exceeding a certain threshold S (indicated by a vertical line in Figure 2)

$$N = N_O \int_{S/Ab}^{\infty} W(g, \omega)\ dg \sim N_o\, e^{-S/Ag_o b}, \qquad (4)$$

where the probability function $W(g, \omega)$ of the spectral amplitude g is approximated by the analytical function

$$W(g, \omega) = \frac{1}{g_o}\ e^{-g/g_o},$$

and

$$g_o(\omega) = \int_{o}^{\infty} g\ W(g, \omega)\ dg$$

is the mean value of $g(\omega)$.

Figure 6 shows the result of counting the number of dots N at different thresholds S (Figure 2) for one thunderstorm at three different frequencies. Because of the relation Equation 4, the dots can be approximated by straight lines (on log paper) which intersect at the point N_o at S = 0. N_o is the total number of atmospherics coming from the thunderstorm within the measured time interval.

The slope of the lines equals

$$A = Ag_0(\omega)\, b(\rho, \omega).$$

Measurements of thunderstorms situated at different distances ρ allow us to separate the value $g_o(w)$ from $b(\rho, \omega)$ (Reference 6). Thus, the amplitude b

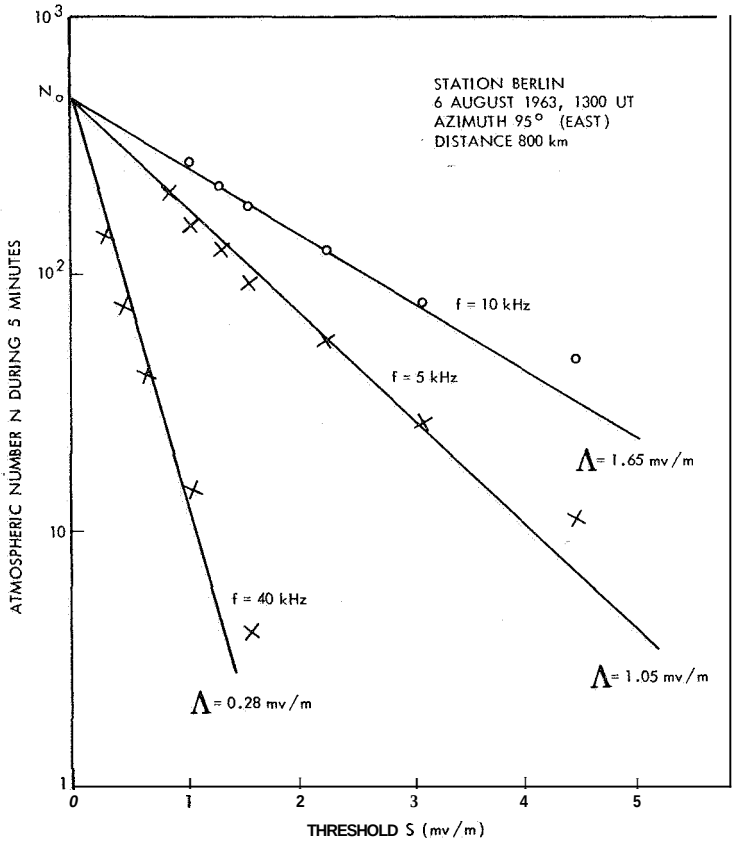

Figure 6 - Number of atmospherics N exceeding threshold S of the receiver for a thunderstorm located at 800 km east from the receiving station, Berlin, at three different frequencies.

of the transmission function of the waveguide and the mean amplitude g_o of the spectral function of the lightning discharges can be derived as functions of distance and frequency.

The equipment described in section 2.3 measures the ratio

$$\frac{b(\rho, \omega_1)g(\omega_1)}{b(\rho, \omega_2)g(\omega_2)}$$

of each atmospheric. The scattering of the points within a cluster in Figure 3 results from the statistical distribution of the values of g for individual atmospherics and from the spaced area of the thunderstorm in which lightning discharges are generated at different distances from the receiver.

Figure 7 shows the ratio of U measured between 6 and 25 kHz to U measured at 8 kHz. The well-known maximum of amplitude around 10 kHz is due to the overlapping of the maximum of the first-order mode and the maximum of g_o in this frequency range. We observe the shift of this maximum to lower frequencies with increasing distance of the thunderstorm.

The group time delay unit (section 2.4) measures the phase difference of the Fourier component in Equation 3,

$$\Delta^2\Phi = \Phi(\rho, \omega_1) + \Phi(\rho, \omega_2) - 2\,\Phi(\rho, \omega_m), \tag{5}$$

where $\Delta^2\Phi$ represents $\dfrac{\delta^2\Phi}{\delta\omega^2}\,\Delta\omega^2$

$$\Phi(\rho, \omega) = \Psi(\rho, \omega) + \psi(\omega),$$

and ω_m, ω_1 and ω_2 are the angular frequencies defined in Equation 1. The difference method is necessary in order to eliminate the large phase value $k_o\rho$ in Ψ ($k_o = \omega/c$ is the wave number in vacuum). $\Delta^2\Phi$ is a measure of the deviation of group velocity from the velocity of light c.

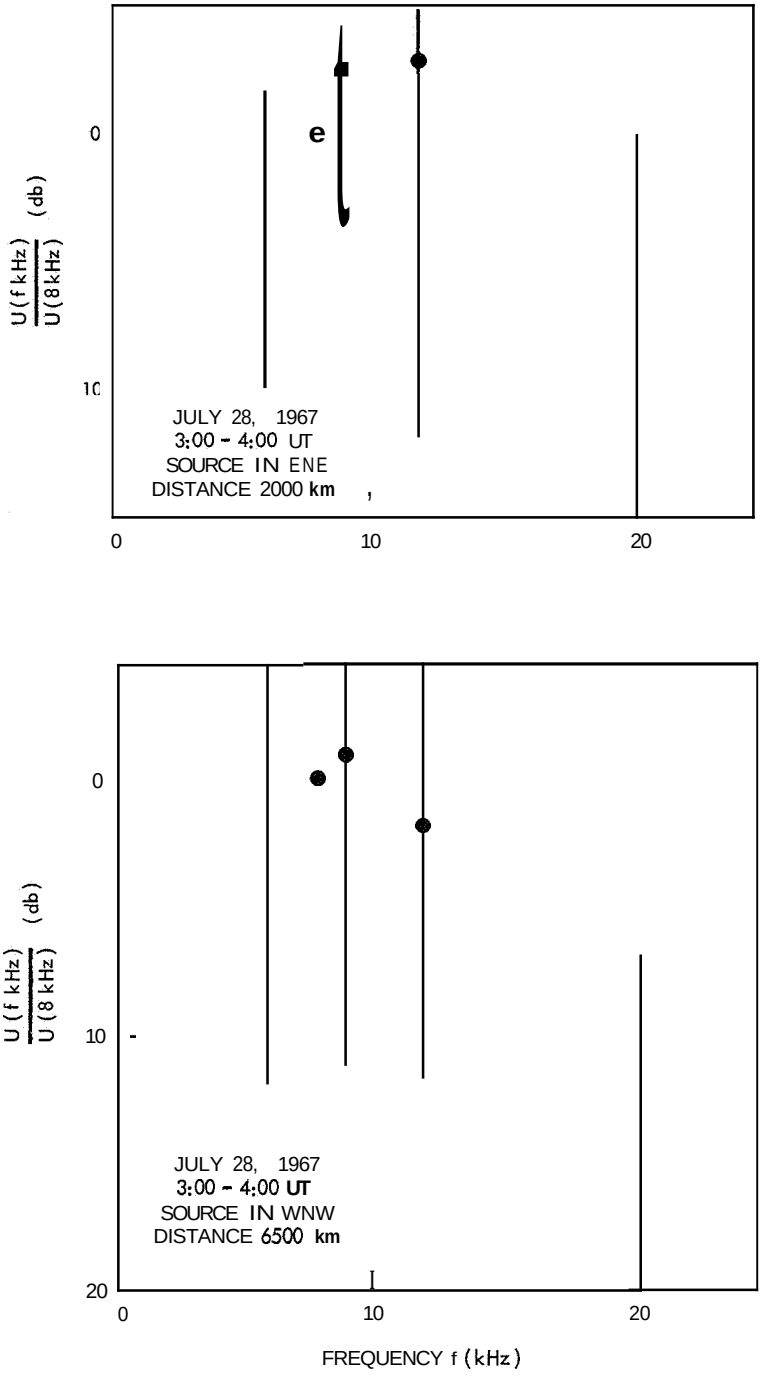

(b)

Figure 7 - Ratio **U (f** kHz)/U (8 kHz) (db) vs frequency for two storms ENE and WNW from receiving station, Stockert. Vertical lines indicate total extension of clusters in Figure **3.** Points are centers of clusters.

The cluster of points in Figure 5 again results from the scattering of the phases of the spectral functions of the single atmospherics and from the different distances of the atmospherics within a thunderstorm. A detailed examination of the group time-delay measurements follows in the next section.

4. Interpretation of the group time delay measurements

The name "group time delay" results from the definition of the time t_{gr} of the propagation of a wave group. The derivative of the spectral phase in Equation 3 with respect to the angular frequency should be zero, i.e.,

$$\frac{\partial}{\partial \omega}(\omega t + \Phi) = 0 .$$

From this, it follows that group time

$$t_{gr} = - \partial \Phi / \partial \omega ,$$

$$\frac{\partial t_{gr}}{\partial \omega} = - \partial^2 \Phi / \partial \omega^2 .$$

Comparing this with Equation 5 and replacing the differentials by differences gives

$$\Delta \omega \Delta t_{gr} = - \Delta^2 \Phi \qquad (6)$$

in agreement with Equation 2.

Group time-delay measurements with a reasonable resolution can be carried out in the 5- to 10-kHz frequency range.

From the theory of VLF propagation, it follows that only the first- and second-order modes are of importance within this frequency range and at distances larger than 500 km.

For a theoretical interpretation of the phase-difference measurements we approximate the transmission function B in Equation 3 by the vertical electric field of a normalized vertical electric dipole (Reference 6). If we consider only the modes of first and second order, the phase of this transmission function is

$$\Psi = -k_o\rho^* + X_1\rho^* + \tan^{-1}\left\{\frac{F \sin\left[\rho^*(X_2-X_1)\right]}{1 + F\cos\left[\rho^*(X_2-X_1)\right]}\right\}, \qquad (7)$$

where

$$X_n + jY_n = k_o(1-S_n) \sim k_o C_n^2/2,$$

$$\rho^* = \rho\,(1 + h/2R),$$

$$F = \frac{D_2}{D_1} e^{-(Y_2-Y_1)\rho^*},$$

$$D_n \sim 1 - \frac{3}{4} C_n^2 .$$

The C_n are the eigenvalues of the modes of order n. The coefficients of their real and imaginary parts are approximately (Reference 6)

$$X_n = \frac{(n - 1/2)^2 \pi^2}{2k_o h^2} - \frac{b_e}{h}, \text{ and}$$

$$Y_n = \frac{a_i (n - 1/2)^2 \pi^2}{k_\theta^2 h^3} + \frac{b_e}{h}, \text{ respectively,}$$

where h is the virtual height of the waveguide, k_θ is the wave number in vacuum, and R is the earth's radius.

The quantity $a_i - \frac{0.34\ \beta^{\alpha-1} f^{2/3}}{h^{a-1}}$ (f in kHz ; h in km)

(a - 4 ; 6 - 65)

is an ionospheric reflection parameter. The factor α, which gives evidence of the increase of reflection during the night, is not very well known. It can be used as an additional parameter. β is the daytime height of the waveguide.

The quantity $b_e = \sqrt{\frac{\epsilon_o \omega}{2\sigma_e}} \sim 3 \cdot 10^{-3} f^{1/2}$ (f in kHz)

is a measure of the influence of the earth's finite conductivity σ_e ($\sigma_e = 3\text{-}10^{-3}$ mhos/m; $\epsilon_o = 8.85 \cdot 10^{12}$ sec/m).

The difference value $A^2\Phi$ of Equation 5 no longer contains the large value $k_o\rho^*$ (see Equation 7). We now disregard $k_o\rho^*$. With the approximations mentioned above, the spectral phase of an atmospheric is

$$\Phi(f, h, \rho, \alpha) = \psi(f) + x - 5.1 \cdot 10^{-5} f^{3/2} h\, x + \tan^{-1}\left\{\frac{e^{-\Gamma x}\sin(8x)}{1 + e^{-\Gamma x}\cos(8x)}\right\}, \quad (8)$$

where

$$x = 58.9\ \frac{\rho^*}{fh^2},$$

$$\Gamma = \frac{3.72}{f^{1/3}}\left(\frac{\beta}{h}\right)^{\alpha}$$

(ρ, h, R in km ; f in kHz).

If we neglect the influence of the second-order mode and of the finite conductivity of the earth (a fair approximation in this frequency range, at least under day time conditions), Equation 8 reduces to

$$\Phi = \psi + x = \psi + \pi^2 c\, \rho^*/8h^2\omega.$$

From Equations 5 and 6 we now find the frequency-normalized group time delay (in μsec/kHz) as

$$-\left.\frac{\Delta t_{gr}}{\Delta f}\right|_{f=f_m} = 2\pi\frac{\Delta^2\Phi}{\Delta\omega^2} = \frac{c\ \rho^*}{16\, f_m^3 h^2}\left\{\frac{1}{\left(1-\frac{\Delta f}{f_m}\right)^2}\right\} + \frac{10^3}{2\pi}\frac{\Delta^2\psi}{\Delta f^2} \qquad (9)$$

(f and Af in kHz; h and ρ^* in **km;** c in km/sec).

The first factor on the right side in Equation 9 is the second derivative of the phase of the first-order mode:

$$2\pi\frac{\partial^2 x}{\partial\omega^2} = \frac{c\ \rho^*}{16 f^3 h^2}. \qquad (10)$$

This factor which dominates the phase behavior in the frequency range between 5 and 10 kHz gives evidence of a simple relation connecting At_{gr}, distance, frequency, **and** virtual height. The additional small value $A^2\psi/\Delta f^2$, which is a pure function of f, can be found by an extrapolation of the data Δt_{gr} (ρ) to the limit $\rho = 1$km.

Figure 8 shows the theoretical values of the normalized group time delay resulting only from the propagation

$$2\pi \left[\frac{\Delta^2 \Phi}{\Delta \omega^2} - \frac{\Delta^2 \psi}{\Delta \omega^2} \right]$$

versus distance ρ with Φ derived from Equation 8 by day (h = 65 km) and by night (h = 85 km). The mid frequency is f_m = 6 kHz, the bandwith is Δf = 1.4 kHz, and the parameter is α = 4. By day, the first mode dominates almost exclusively at distances greater than 1000 km; at night the influence of the second-order mode becomes small at distances greater than about 4000 km. The dashed lines show values of $2\pi A^2 x/\Delta\omega^2$.

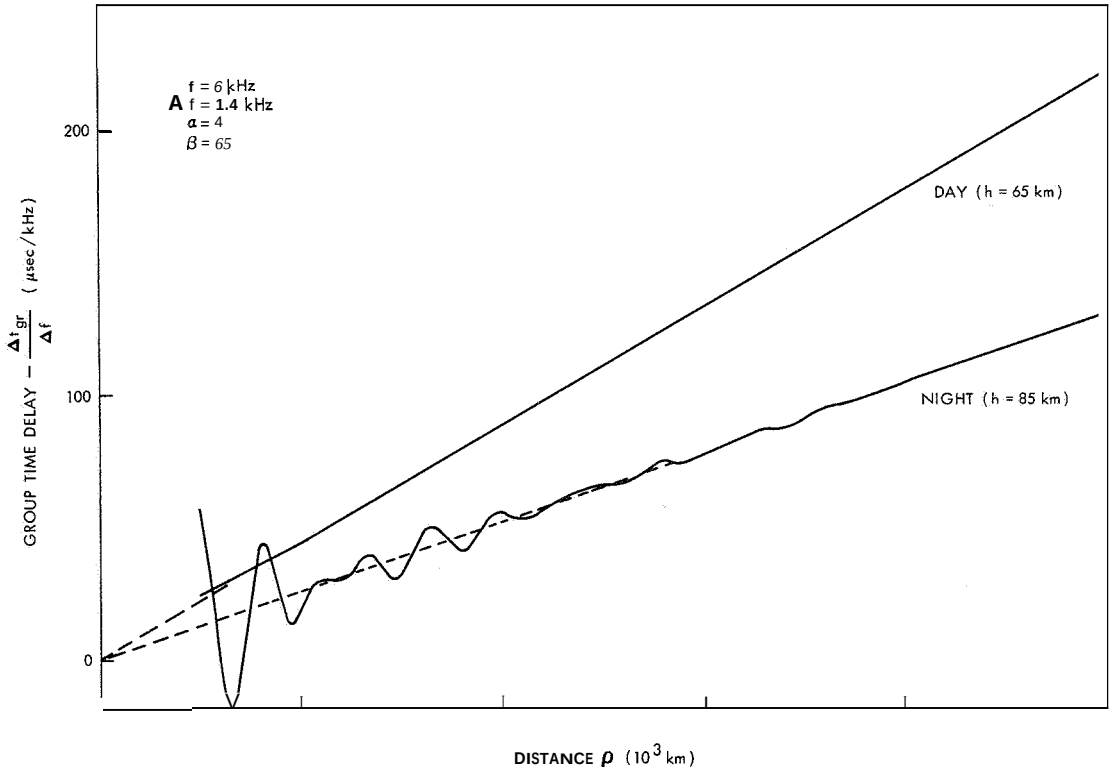

Figure 8 - Theoretical values of group time delay due to the propagation waveguide versus distance by day and at night. The dashed lines are calculated from the first propagation mode.

Theory shows that Equation 9 is a fair approximation of the group time delay in this frequency range.

Figure 9 shows the diurnal variation of the normalized group time delay (30-minute means) measured from a prolonged thunderstorm at 6800 km distance in a WNW direction from the observing station at Stockert near Bonn, Germany.

The thunderstorm disappeared at 1900 UT, May 10. Because of the greater attenuation of the electromagnetic waves in the daytime waveguide, the nighttime values of the group time delay are much more easily observed than the daytime values.

In Figure 10 the nighttime group time delay values at f = 6 kHz and $\Delta f = 1.4$ kHz of 20 prolonged thunderstorms observed between April 20 and May 10, 1967, and located mainly in a west direction, are plotted against their distance ρ from the receiving station Stockert. The location of the thunderstorms was determined from the TV-cloud pictures of the ESSA 5 satellite.

A linear relationship between Δt_{gr} and ρ is suggested by Equation 10. From the slope of the curve in Figure 10 we can derive, with the help of Equation 9, a nighttime value of the virtual height of the waveguide as

$$h_N = 70 \text{ km},$$

which is significantly lower than the nighttime values observed at short distances and higher frequencies (References 6 and 7).

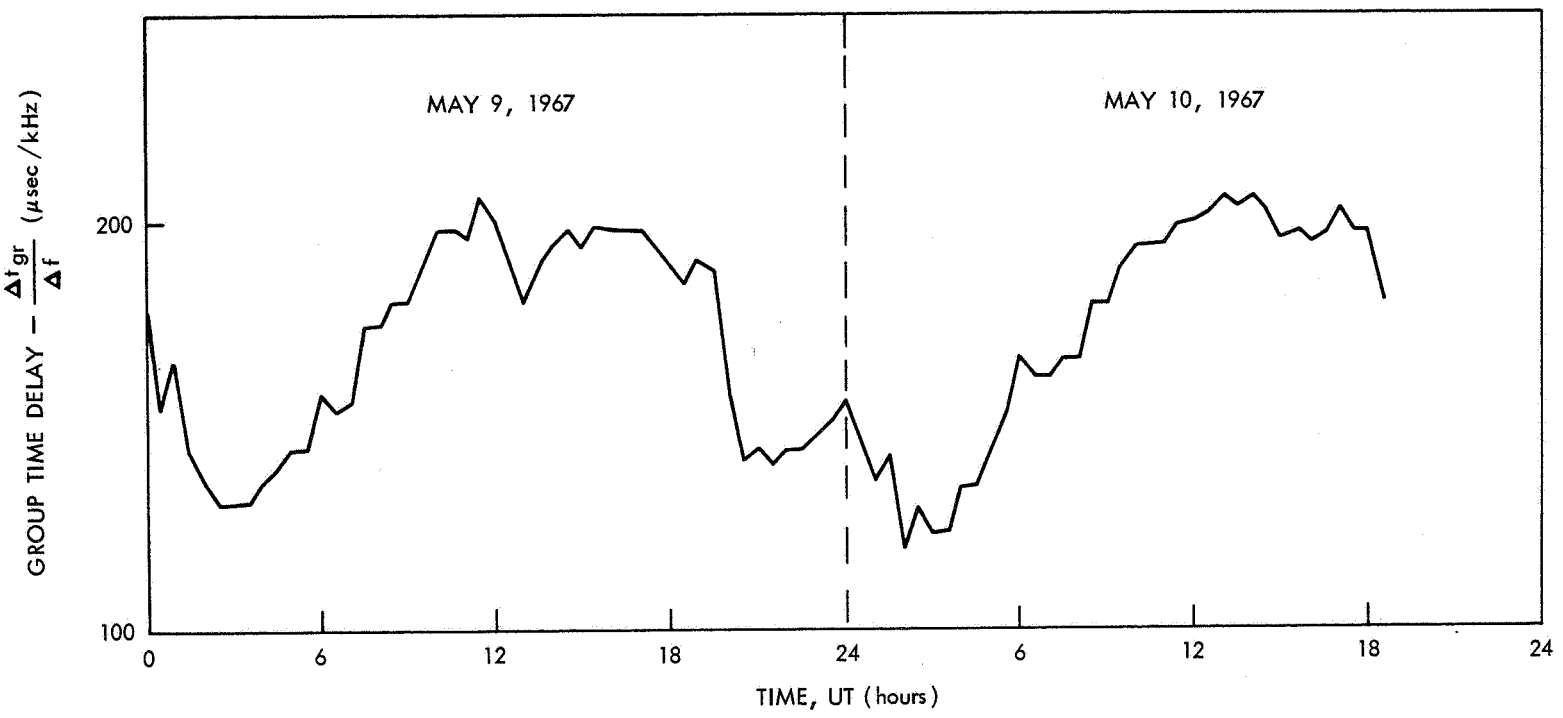

Figure 9 - Measured group time delay versus time for a thunderstorm located at 6800 km WNW from the receiving station Stockert.

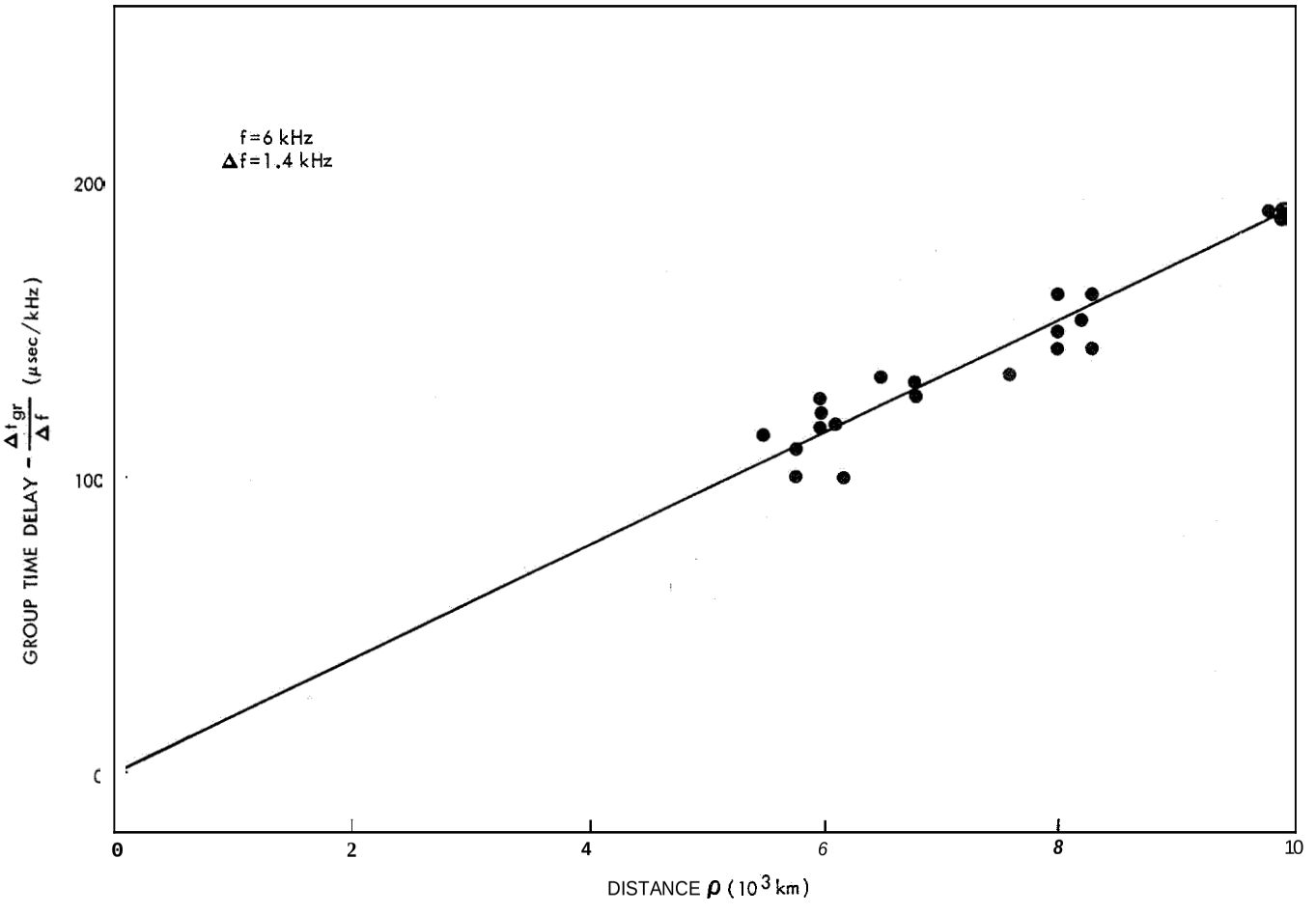

Figure 10 - Nighttime group time delay versus distance measured in April and May, 1967 from thunderstorms mainly located west of the receiving station Stockert. The firm line is the theoretical value of the first mode with h_N = 70 km.

Figure 11 shows the ratio

$$R = \frac{\Delta t_r(\text{night})}{\Delta t_{gr}(\text{day})}$$

between the nighttime minimum and daytime maximum value of the group time delay of the same 20 thunderstorms that are examined in Figure 10 plotted against $\Delta t_{gr}(\text{night})/\Delta f$. The arrows indicate upper limit values. With a mean value of R = 0.64 from Figure 11 we obtain a daytime value

$$h_T = 56 \text{ km}$$

of the virtual height of the waveguide which is again significantly lower than the observed values for short propagation paths and at high frequencies (References 6 and 7), but fits well with phase measurements for long propagation paths (Reference 8).

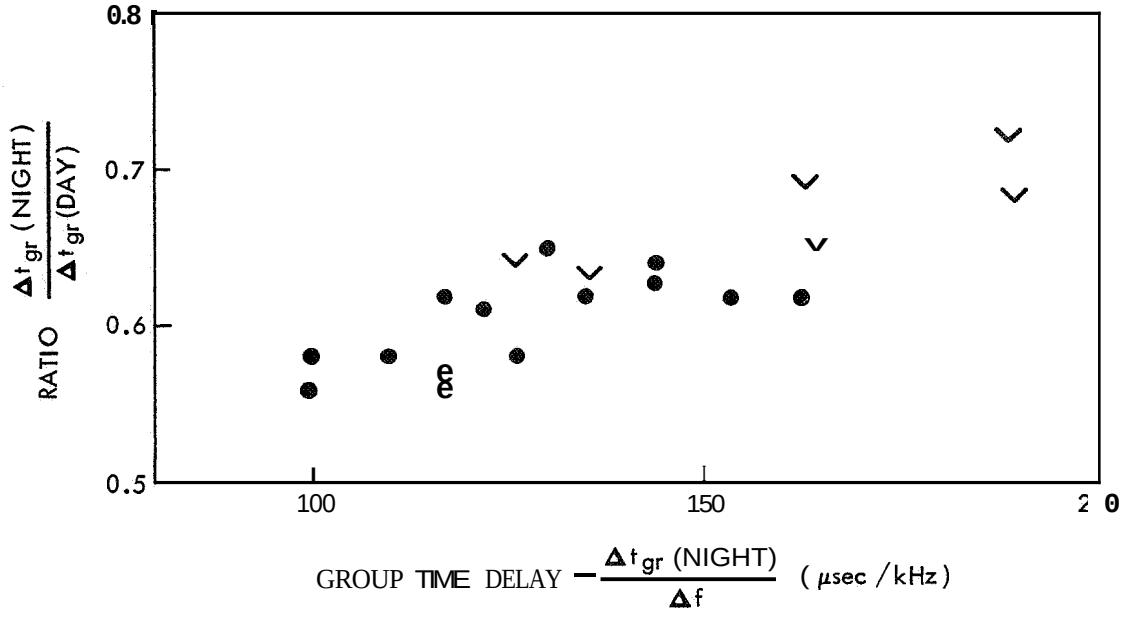

Figure 11 - Ratio Δt_{gr} (night) / Δt_{gr} (day) versus nighttime group time delay measured in April and May, 1967, for different thunderstorms located mainly west of the receiving station Stockert.

Figure 12 shows the group time delay of two distant thunderstorms versus $1/f^3$, verifying the inverse third-power law of Equation 10.

In Figure 10 and Figure 12 the straight lines approximating the measured values go nearly through the origin at $\rho = 1$ km or $1/f^3 \rightarrow 0$. This means that the spectral function of the atmospherics ($\partial^2\psi/\partial f^2$ in Equation 9) value seems to be very small and thus is difficult to determine. Our measurements show that Equation 10 describes sufficiently well the phase behavior of VLF waves below 10 kHz. Group time delay measurements in this frequency range can therefore serve as an excellent tool for the location of distant thunderstorms,

5. Concluding remarks

This paper gives a short description of an equipment which measures spectral amplitude, amplitude ratio, and group time delay of atmospherics versus their azimuth in the VLF range, The amplitude measurements are interpreted by a statistical method that gives the amplitude of the propagation function of the waveguide as a function of frequency and distance and gives the mean spectral amplitude of the lightning discharges at their origin.

By the amplitude-ratio measurements, the frequency and spatial-dependent behavior of the field strength within the VLF range can be determined.

The group time delay is proportional to the second derivative of the spectral phase of the atmospherics with respect to the angular frequency. Its theoretical value

$$-\Delta t_{gr} = A\rho/f^3h^2 \qquad (11)$$

depends on distance ρ, frequency f, and virtual height h of the waveguide. This relation is verified by measurements of distant and prolonged thunderstorms.

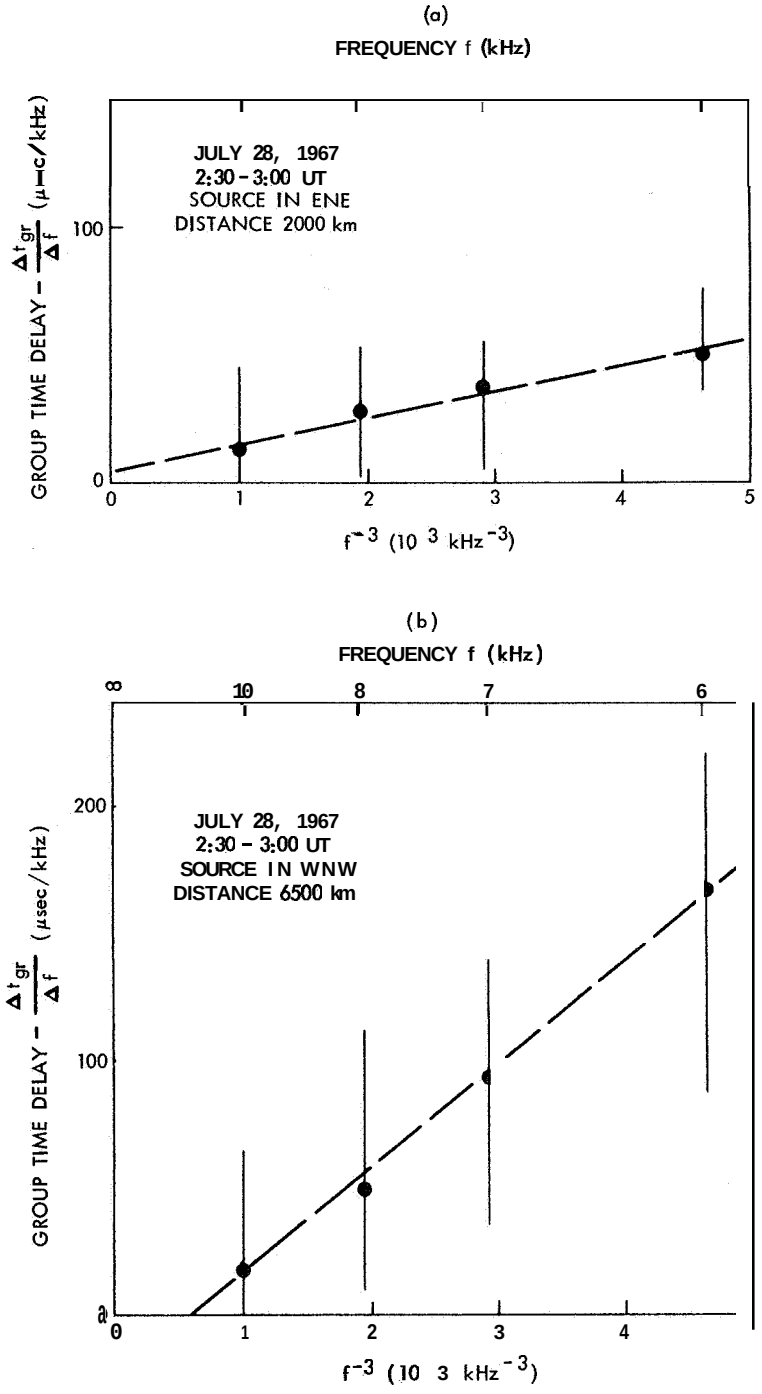

Figure 12 - Group time delay vs $1/f^3$ for two storms ENE and WNW from receiving station, Stockert. Vertical lines indicate total extension of clusters in Figure 5. Points are centers of clusters. (Bandwidth Af = 1.4 kHz.)

Acknowledgement

I am very indebted to Mr. Ferguson, National Environmental Satellite Center of ESSA, Washington, D. C., who kindly provided me with the TV pictures of the ESSA 5 satellite, and gave me invaluable help in reading cloud pictures.

REFERENCES

1. Glade, P., Lauter, E. A., and Schäning, B., "Sommerliche Tagesgnge des atmosphärischen Störpegels auf Längstwellen in verschiedenen Breiten," Gerland's Beitr. Geophysik 73: No. 3, 137, 1964.

2. Taylor, W. L., and Jean, A. G., "Very-low-frequency radiation spectra of lightning discharges," Journ. Res. Nat. Bur. Stds. 63D (2): 199–204, Sept. Oct. 1959.

3. Pierce, E. T., "Atmospherics - Their characteristics at the source and propagation," in "Progress in Radio Sciences 1963–1966," Amsterdam: Elsevier Publ. Comp.

4. Horner, F., "Atmospheric noise and its influence on communications," in "Progress in Radio Sciences 1963–1966," Amsterdam: Elsevier Publ. Comp.

5. Heydt, G., "Peilanlagen zur Messung von spektralen Amplitudenverteilungen, Amplitudenverh'riltnissen und Gruppenlaufzeitdiff erenzen von Atmospherics," Technischer Bericht des Heinrich-Hertz-Instituts, Berlin-Charlottenburg, 1967.

6. Volland, H., "Die Ausbreitung langer Wellen," Braunschweig: Vieweg Verlag, 1968.

7. Frisius, J. , "Observations of diurnal amplitude and phase variations on a 16 kHz transmission path and their interpretation by a simple propagation model," XIIIth Symposium of AGARD held in Ankara, Turkey, October, 1967.

8. Westfall, W. D. , "Prediction of VLF phase change and solar flare effects," J. Geophys. Res. 66: 2733, 1961.